Monitoring landslide displacements by using ground-based synthetic aperture radar interferometry: Application to the Ruinon landslide in

JOURNAL OF GEOPHYSICAL RESEARCH, VOL. 108, NO. B8, 2387, doi:10.1029/2002JB002204, 2003

Monitoring landslide displacements by using ground-based synthetic aperture radar interferometry: Application to the Ruinon landslide in the Italian Alps

Dario Tarchi
European Commission, Joint Research Centre, Institute for the Protection and Security of the Citizen, Ispra, Italy

Nicola Casagli and Sandro Moretti
Earth Sciences Department, University of Florence, Florence, Italy

Davide Leva and Alois J. Sieber
European Commission, Joint Research Centre, Institute for the Protection and Security of the Citizen, Ispra, Italy

Received 16 September 2002; revised 27 January 2003; accepted 17 April 2003; published 20 August 2003.

[1] Synthetic aperture radar (SAR) data are collected by a ground-based radar system forming the synthetic aperture by the sliding of the antennas on a linear rail. Coherent SAR processing converts the raw data into a complex image. The phase of each image pixel contains information on the target-sensor distance and can be exploited as a ranging tool. The interferometric technique, based on the comparison between paired and coherent SAR images taken at different times, permits the quantitative extraction of this information, thus allowing the monitoring of the morphological changes. The portable device used in this application was developed by the Joint Research Center, Ispra, Italy, specifically for measurements in the field. It is known as Linear SAR, and it is able to provide 17 GHz measurements with a 2.8 m synthetic aperture. A measurement campaign, lasting about 1 week, was performed between July and August 2000 for monitoring superficial displacements at the Ruinon landslide, a 30 million m^3 rockslide in the Italian Alps. Two sequences of interferograms are presented and discussed. The interpretation of the sequences has allowed us to derive multitemporal deformation maps of the test area, thus showing the entire displacement field of those landslide sectors characterized by higher radar reflectivity and coherence. Displacement rates up to 1.2 mm h^{-1} have been measured with a pixel resolution of 5 m and a measurement precision of 0.75 mm. The results have been validated by using ground truth data obtained through automatic extensometers and topographic measurements. Discrepancies are limited to a few millimeters. *INDEX TERMS:* 0694 Electromagnetics: Instrumentation and techniques; 1204 Geodesy and Gravity: Control surveys; 1824 Hydrology: Geomorphology (1625); 1894 Hydrology: Instruments and techniques; 9810 General or Miscellaneous: New fields (not classifiable under other headings); *KEYWORDS:* remote sensing, interferometry, radar, landslide, monitoring, ground-based DInSAR

Citation: Tarchi, D., N. Casagli, S. Moretti, D. Leva, and A. J. Sieber, Monitoring landslide displacements by using ground-based synthetic aperture radar interferometry: Application to the Ruinon landslide in the Italian Alps, *J. Geophys. Res.*, *108*(B8), 2387, doi:10.1029/2002JB002204, 2003.

1. Introduction

[2] One of the main applications of synthetic aperture radar (SAR) interferometry (InSAR) is the monitoring of natural hazards, in particular of those phenomena producing ground displacements. According to the type of platform employed, the natural phenomena which can be studied and their spatial and temporal scale of observation are different.

[3] Several examples prove the effectiveness of differential SAR interferometry from satellite platforms for measuring ground displacements over wide areas due to different causes, such as earthquakes, volcanic activity, glacier motion, and subsidence related to underground mining or fluid extraction [*Gabriel et al.*, 1989; *Massonnet et al.*, 1993, 1994, 1995; *Goldstein et al.*, 1993; *Peltzer et al.*, 1994; *Carnec et al.*,1994, 1995; *Williams et al.*, 1998; *Ferretti et al.*, 1999a, 2000].

[4] Another important field of application is the monitoring of slope movements or landslides. Several examples of successful applications of satellite SAR sensors have been recently published in cases of large, slow-moving landslides [*Achache et al.*, 1995; *Prati et al.*, 1995; *Fruneau et al.*, 1996; *Carnec et al.*,1996; *Singhroy et*

0148-0227/03/2002JB002204$09.00

al., 1998; *Ferretti et al.*, 1999b, 2001; *Rott and Siegel*, 1999; *Wasowski and Gostelow*, 1999; *Rott et al.*, 1999, 2000; *Kimura and Yamaguchi*, 2000; *Singhroy and Mattar*, 2000; *Refice et al.*, 2000; *Rizzo and Tesauro*, 2000].

[5] A landslide is a mass of rock, debris, or earth which moves down a slope due to gravity [*Cruden*, 1991]. Despite this simple definition, a landslide is a complex phenomenon [*Cruden and Varnes*, 1996]. It is characterized by five fundamental mechanisms of movement (fall, topple, slide, spread, and flow) and their combinations. Landslides can occur on a range of slopes varying from vertical cliffs (falls) to horizontal land (spreads), in which the material involved can range in size and consistency from hundreds of millions of cubic meters of solid rock to single particles of earth or debris. The rate of movement ranges over more than ten orders of magnitude, from imperceptible creeping (velocity $<10^{-10}$ m s^{-1}) to catastrophic failures (velocity >10 m s^{-1}), while the material can move as a whole like a solid block or can flow like a fluid, depending on the water content and other factors. In addition, landslide activity can vary in space and through time and even between different parts of the same displaced mass.

[6] Owing to this complexity, the satellite platforms presently operational are, in general, of limited utilization for landslides since their characteristics, such as the incidence angle, the spatial resolution, and the time interval between successive passages, are not optimal compared to the particular spatial and temporal pattern of movements. In those cases where the landslide has particular characteristics, such as the coverage of a small area, a fast-moving rate of displacement, and an occurrence on steep slopes or within narrow valleys, the use of ground-based sensors represents a valid complement to satellite sensors. Moreover, in some situations they are the only sensors which can be deployed in order to guarantee the necessary flexibility and adaptability needed for each specific case.

[7] This paper focuses on an application of ground-based differential InSAR (GB-DInSAR) using portable ground-based instrumentation to produce deformation maps of the observed slope. The technique was originally proposed by the authors for the monitoring of a variety of man-made structures and has already been validated through laboratory and field tests in operational conditions on an arch dam, on a bridge, and on a slope affected by underground mining activity and gravitational slope deformations [*Tarchi et al.*, 1997, 1999, 2000a, 2000b; *Pieraccini et al.*, 2000a, 2000b].

[8] A research program funded jointly by the Italian Space Agency and by the National Research Council Group for Hydro-Geological Disaster Prevention and supported by the Italian Department of Civil Protection started in 1999 with the aim of exploring the applicability of GB-DInSAR for monitoring landslides. In the framework of this ongoing program, GB-DInSAR has been tested on a series of landslides with different types of movement, different materials, different rates of movement, and different distributions/styles of activity.

[9] A first application of GB-DInSAR to the "landslide problem" has been performed by *Beatrizotti et al.* [2000] on the Airolo landslide, a complex slope movement probably originated by a slow toppling of rock blocks. In that case, only the acquisition of the first "reference image" is described, but no interferograms, showing displacement fields, are produced.

[10] Here a new specific application to a landslide site is described. We considered a large rockslide in the Italian Alps, where the presence of an independent monitoring system allowed us to validate the results through "ground truth" measurements. The preliminary results of this campaign, carried out between July and August 2000, have been discussed in three short notes by *Atzeni et al.* [2001a, 2001b, 2003], but they are here presented in detail and thoroughly discussed. A parallel paper [*Tarchi et al.*, 2003] discusses the results of another campaign carried out, in October 2000, on the Tessina landslide, a large, complex earth slide/flow located in the Italian eastern Alps.

2. Differential SAR Interferometry (DInSAR)

[11] The SAR technique is employed to obtain high-definition microwave images by using antennas of relatively small size mounted on spaceborne, airborne, or ground-based carriers [*Curlander and McDonough*, 1991]. The antenna synthesis is obtained by moving the sensors, usually along a straight trajectory, and by repeating radar measurements perpendicularly to the movement direction at selected spatial intervals. The data processing results in an image with a spatial resolution approximately equal to that obtainable through a real antenna with a dimension equal to the segment of trajectory covered by the sensor.

[12] The spatial resolutions of the images typically range from 10 to 25 m for the current operational satellites and from 1 to 3 m for the most advanced airborne sensors. Using ground-based sensors, the resolution depends on the distance between the sensor and the target area; usually, it is possible to obtain a resolution of the order of a few centimeters at a distance of some tens of meters and a resolution of a few meters at a distance of some kilometers.

[13] Each pixel of a complex SAR image is characterized not only by its radiometric amplitude, expressing the target reflectivity at the frequency of observation, but also by its phase, depending on the target-to-sensor distance and on the dielectric properties of both the target and the medium where the electromagnetic wave propagates. In general, in a single SAR image these two contributions cannot be separated, and moreover, only the principal value of the electromagnetic phase of each pixel can be measured. This is the reason why a single SAR image is not directly usable in practical applications such as topography estimation and monitoring of ground displacements.

[14] The above mentioned problems can be solved, under particular assumptions, by using coupled SAR images of the same scene obtained through identical measurement parameters. The quantitative comparison between a pair of complex SAR images produces an interferogram showing the phase difference between the two images. In this way, dielectric effects can be minimized or cancelled out, provided that they were similar at the moments of the two acquisitions.

[15] The residual phase difference can then be related, pixel by pixel, to topography and/or to relative displacements of the corresponding portions of the observed area. The topographic effect is dependent on the baseline, namely, the perpendicular distance between the paths described

by the sensor during data acquisition, and disappears for a pair of images acquired from exactly the same location. This condition (zero baseline) is the ideal arrangement for the application of InSAR aimed to measure ground displacements. Since the zero baseline condition is almost impossible to be realized with spaceborne and airborne platforms, an additional step is necessary in order to separate the two above mentioned effects and to extract information on displacements. The technique is referred to as differential interferometry (DInSAR) and, basically, subtracts a second interferogram, which is considered to contain only topographic effects, from the first one. To this aim, two alternative methods have been proposed. The former is referred to as three-pass interferometry [*Zebker and Goldstein*, 1986], which uses a third image. The latter, referred to as digital elevation model (DEM) extraction method [*Rosen et al.*, 2000], generates a synthetic interferogram by using an existing DEM of the observed area and the precise knowledge of the trajectories (orbital parameters) of the sensor during the acquisition of the paired images.

[16] On the other hand, with a ground-based platform, the ideal condition of zero baseline can usually be met, and a couple of images are sufficient to generate a topography-free interferogram and, finally, to derive information on displacements. For the sake of simplicity we refer to this specific application of InSAR using a ground-based system as GB-DInSAR.

[17] Independently, for both the platform and the specific method, whenever the application of DInSAR is monitoring movement, the final product can be referred to as a displacement map having the following general characteristics: (1) measured displacements referring to the component of the real displacement along the line-of-sight (LOS) of the SAR system and to the time span between the acquisitions of the SAR images; (2) spatial resolutions equal to those of the original SAR images; the resolution could degrade if spatial averaging is applied at a step of the processing chain; and (3) accuracy in measuring displacements, usually a fraction of wavelength.

[18] Note that the typical ambiguity in the interpretation of the phase measurement is only partially solved since the relative displacement of each pixel cannot exceed half of a wavelength. Since this criterion holds for adjacent pixels, displacements of even several wavelengths can be correctly measured, provided that they are characterized by a ''smooth'' spatial distribution regarding a large number of pixels. An unambiguous interpretation of the results can be achieved by applying an additional processing step, referred to as ''phase unwrapping'' [*Goldstein et al.*, 1988; *Fornaro et al.*, 1996].

3. Description of the Test Site

[19] The Ruinon (literally, ''huge ruin'') landslide is one of the most hazardous slope movements in the Italian Alps. It is located in Valfurva (Middle Valtellina), near the village of Bormio, in the Rhaetian Alps (Figure 1). The landslide is currently active, and its continuous movements affect an estimated volume of rock of ~30 million m^3, representing a serious threat to human lives and socioeconomic activities in the area. Its rapid collapse would destroy the road connecting the well-known tourist resorts of Bormio and Santa Caterina Valfurva and, most importantly, would block the Frodolfo stream, with the probable formation of a highly unstable landslide dam.

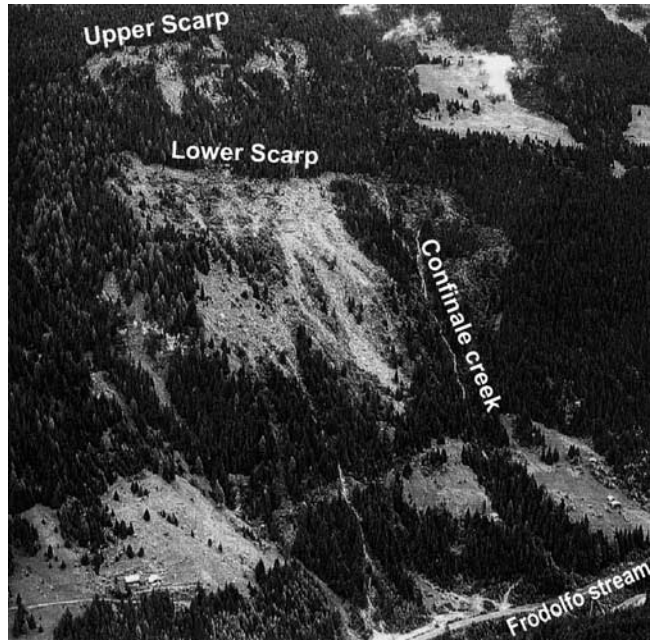

Figure 1. Aerial picture of the Ruinon rock slide.

[20] The geological aspects of the landslide have been studied in detail by *Del Piccolo* [1999], G. Crosta et al. (unpublished manuscript, 1999), and *Agliardi et al.* [2001]. The landslide is located in the lower portion of a southwest facing slope (azimuth of the dip direction = 240°N), with an average inclination of 36°, on the hydrographic right of the Frodolfo stream (Figure 2).

[21] The slope consists of pre-Permian metapelites (phyllites), belonging to the Upper Austroalpine basement of the Campo-Ortles Nappe, and is locally covered by glacial deposits and debris produced by rockfalls. The schistosity of the metapelites dips toward 35°N, with an inclination of 22°. The landslide, which has a total length of 770 m and a width of 410 m, is characterized by two main scarps oriented northwest-southeast, parallel to the main fracture system: The ''upper scarp'' is located at an elevation of ~2100 m above sea level (asl), the ''lower scarp'' at ~1900 m asl. The southeastern border of the landslide is abruptly cut by the Confinale creek, a right-hand tributary of the Frodolfo, the course of which is controlled by a northeast-southwest master joint.

[22] The geological section of the slope in Figure 3 shows a possible interpretation of the landslide geometry and movement mechanism. The section is based on four deep boreholes, equipped with inclinometers, showing the presence of weak and cataclastic zones at depths of >90 m (G. Crosta et al., unpublished manuscript, 1999).

[23] In recent work, *Agliardi et al.* [2001] interpret the landslide within the broader context of a large-scale, Sackung-type, deep-seated slope gravitational deformation, affecting the entire slope between the Cavallaro and the Confinale valleys in Valfurva from an elevation of ~3000 m asl to the valley bottom and with an areal extension of ~6 km^2.

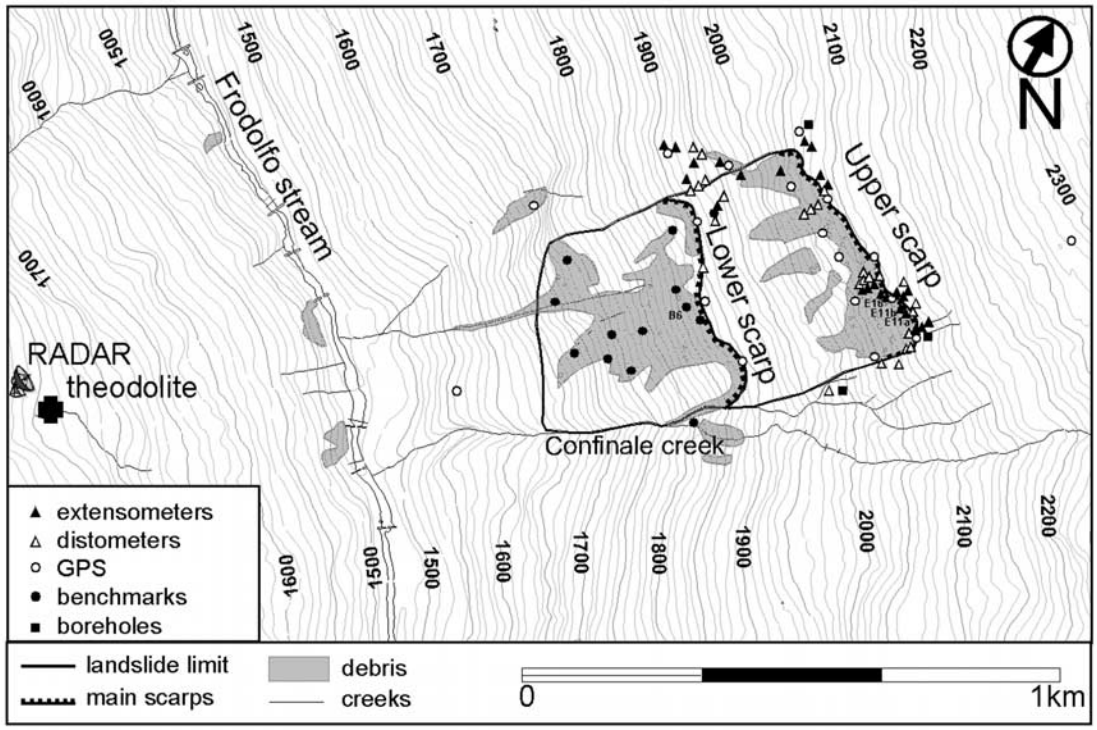

Figure 2. General plan showing the main geomorphic elements and the location of monitoring instrumentation. The position of the radar is also shown. Labels E11a, E11b, E16, and B6 indicate the sensor used for data validation.

The entire slope is monitored by the Geological Monitoring Center of the Lombardia Regional Administration through an extensive network composed of a series of extensometer and distometer sensors, part of which are equipped for real-time data acquisition and transmission, plus survey-mode GPS and topographic benchmarks. Details on the monitoring instrumentation are given in Table 1, whereas the location of the main active control points is shown in Figure 2.

[24] The recorded movement pattern is typical of a ''rock slide'' mechanism, with a deep-seated sliding surface. The most active sectors of the landslide are located in the southeastern portions of the two main scarps. The upper scarp is characterized by maximum movement rates of $\sim$6 mm d^{-1}

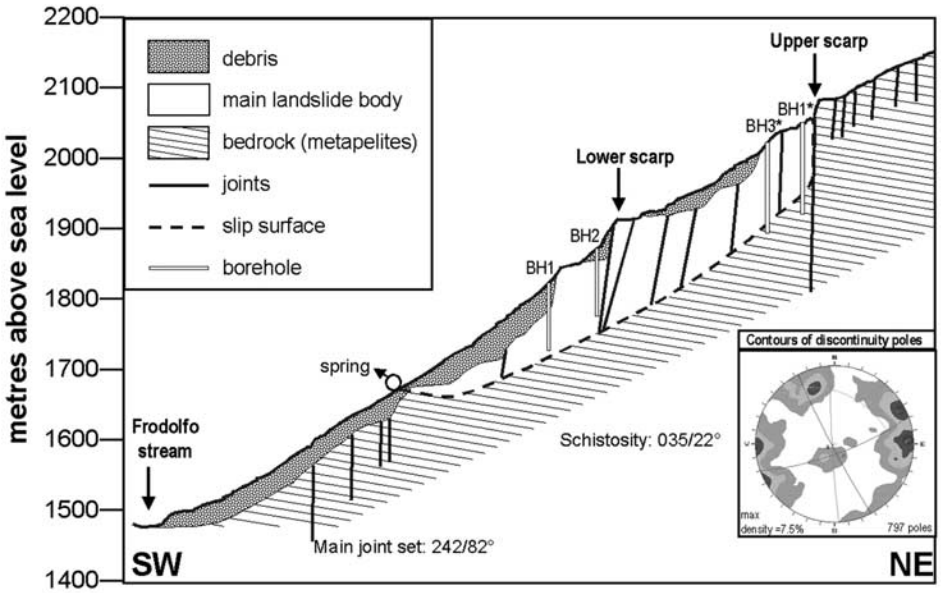

Figure 3. Interpretative cross section with a hypothesis of the landslide geometry.

Table 1. Main Characteristics of the Network for Monitoring Surface Displacements[a]

Label	Type of Instrument	Number of Control Points	Frequency of Observations[b]
E	automatic extensometers	16	4
D	manual distometers	71	1–7
B	terrestrial geodetic measurements	16	1
GPS	Global Positioning System	18	1

[a]The monitoring network was installed by the Geological Monitoring Centre of the Lombardia Regional Administration.
[b]Systems E, D, B, and GPS are measured in days, hours, months, and years, respectively.

in its southeast sector (on the right in Figure 1); abrupt accelerations occur after major rainfalls, with a delay of ~10 days with respect to the rainfall peak (G. Crosta et al., unpublished manuscript, 1999). Scarce information is available on the displacement rates within the lower scarp since no automatic instrumentation has been installed; first data from topographic and GPS surveys seem to suggest velocities as high as 30 mm d^{-1}.

[25] A DEM of the landslide with a 5 × 5 m resolution was built by digitizing topographic contour lines on a 1:2000 map produced by the Regione Lombardia (Figure 4). The projection of the radar image on the DEM is necessary for a correct interpretation of the displacement maps.

4. Materials, Methods, and Measurement Campaign

[26] The system employed is a portable SAR device known as Linear SAR (LISA), specifically designed and implemented by the Joint Research Centre, Ispra, Italy, for in-field use. A scheme of the hardware is provided in Figure 5. The microwave component of the system is composed of a continuous-wave, stepped-frequency scatterometer based on a network analyzer which includes a signal source from 30 kHz to 6 GHz. An additional module from coherent up-and-down frequency conversion allows measurements in the frequency band from 14 to 18 GHz. The antenna synthesis is obtained by moving a motorized sled, hosting the antennas and other microwave components, along a 2.8 m long linear rail system [*Rudolf et al.*, 1999; *Rudolf and Tarchi*, 1999]. A drawback of the use of a ground-based system is the limitation on the maximum extent of the synthetic aperture, which is usually much smaller than the azimuth extent of the image area. As a consequence, the azimuth resolution is far from optimal, i.e., the resolution which can be attained when the synthetic aperture is equal to the footprint of the antenna of the system. Attainable resolution can be even an order of magnitude less than the optimum but still sufficient for many applications. In addition, the azimuth resolution is not constant, decreasing with the range distance and the lateral position of the image pixel with respect to the center of the synthetic aperture.

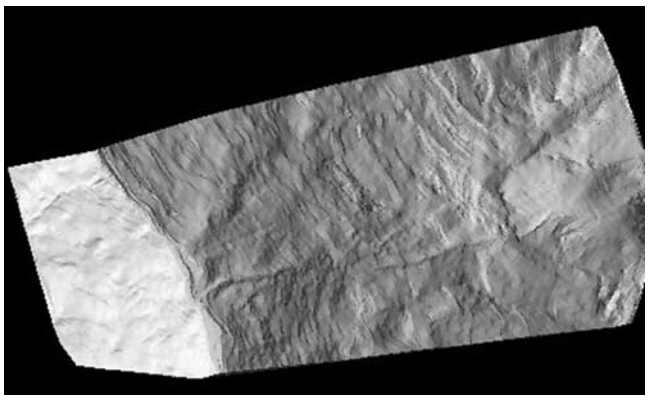

Figure 4. Shaded relief of the test site based on a digital terrain elevation model with pixels of 5 × 5 m.

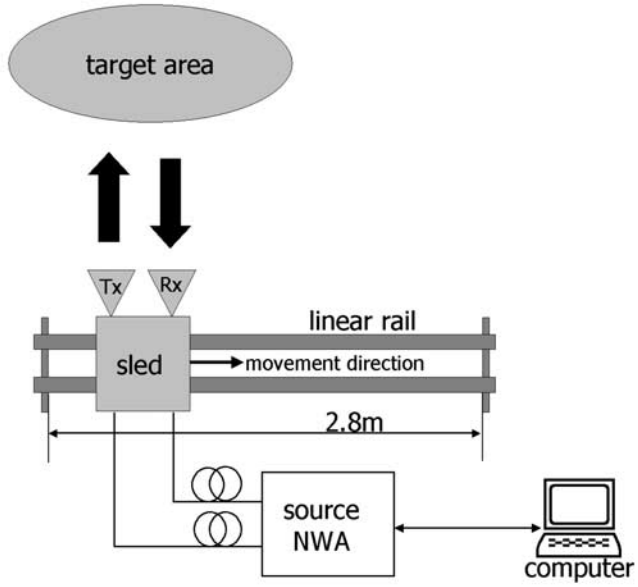

Figure 5. Scheme of the hardware components of the Linear SAR (LISA). Tx, transmitting antenna; Rx, receiving antenna; and NWA, network analyzer.

[27] Measurements were undertaken at the test site using the maximum synthetic aperture length of 2.8 m with an azimuth step of 0.7 cm, an observation frequency band from 16.80 to 16.88 GHz, and a frequency step of 50 kHz. The transmitted power was ~25 dBm (≈300 mW).

[28] The measurement campaign was carried out in the period between 25 July 2000 and 2 August 2000. The instruments were rigidly fixed on a stable support (Figure 6) on the slope facing the Ruinon landslide (Figure 2), at an average distance of 1.3 km, in a site accessible only with off-road vehicles and devoid of utilities (electricity, telecommunications, etc.). The electricity was supplied by a gasoline generator and then was stabilized by UPS. Data were collected, stored, and processed on laptop computers directly in the field.

[29] The main characteristics of the measurement system in operational conditions along with measurement parameters are summarized in Table 2. In accordance with the selected parameters, the range resolution is ~2 m while the azimuth resolution ranges from 3 to 5 m.

[30] Image acquisitions were repeated at time intervals of ~35 min from the same position (zero baseline). The overall duration of the campaign was 7 days (between 27 July 2000 and 2 August 2000) since the first few days were dedicated to solving problems caused by the lack of facilities in the

Figure 6. The portable version of LISA used in the test site: (a) detail of the antennas and (b) field arrangement of the instrumentation.

sites. The time span between successive acquisitions was selected by considering the track record of displacement rates of the landslide and, also, the necessity of repeating measurements in constant conditions of soil moisture and vegetation cover.

5. Data Processing

[31] The SAR images are obtained from the raw data collected by the LISA system after a data processing procedure which includes the following.

[32] (1) Calibration was used to eliminate systematic errors introduced by the system by using sets of parameters retrieved from the periodical calibration measurements of a metallic disc placed at a known orientation and distance from the LISA [*Wiesbeck and Kähny*, 1991].

[33] (2) Focalization involves the reconstruction of the correct two-dimensional distribution of backscattered energy of the observed scenario. In order to overcome, in an efficient way, the specific problems posed by an azimuth extent much larger than the synthetic aperture, a tailored time-domain SAR focusing algorithm has been developed

Table 2. Main Characteristics of the System in the Operational Condition at the Test Site

Parameter	Value
Frequency band, GHz	16.80–16.88
Frequency step, kHz	50
Frequency points	1601
Aperture, m	2.80
Azimuth step, mm	7
Azimuth points	401
Polarization	VV
Transmitted power (approximate), dBm	25
Target distance (average), m	1300
Spatial resolution (range), m	2
Spatial resolution (cross range), m	4
Measuring time per image, min	35
Total time interval, days	7
Number of collected images	124

based on the approach of *Fortuny and Sieber* [1994]. Such an algorithm can perform the focusing on an arbitrary set of points, thus allowing one to incorporate, at this stage, the radar image georeferencing. In fact, this can be easily accomplished provided that a DEM of the target area is available and that the position of the radar system with respect to the target area is known. In this condition the resulting image is directly referred to the coordinate system of the DEM without the typical distortion of the SAR products.

[34] (3) In order to minimize those artifacts due to moving objects on the observed scene (such as wind-blown vegetation), groups of three or four images, sequentially acquired, were coherently averaged. In this way, defocusing effects are minimized and the signal-to-noise ratio of the final image is increased. Consequently, the effective time interval between image pairs used to form the interferograms ranges between 105 and 140 min.

[35] (4) The analysis of coherence has been applied to individuate those areas where the phase measurement is disturbed (e.g., vegetation movement during image acquisition), and consequently, it is unsuitable for the assessment of distance variations. Pixels with low coherence, usually corresponding to vegetated areas, have been excluded from the images by applying a two-level mask.

[36] In order to estimate the measurement precision, the phase difference distribution in stable areas has been analyzed. This distribution shows a mean value of $-4°$, very close to the theoretical value of $0°$, whereas the standard deviation, converted in displacement by considering the central frequency of observation, is equal to 0.75 mm. This figure has been assumed as the theoretical precision of the system under the specific operational conditions in the field.

[37] After the whole data processing chain the image resolution is reduced to $\sim 4 \times 6$ m (range $\times$ azimuth). This is due, in particular, to the windowing of the radar raw data required by the SAR processing algorithm.

6. Measurement Results

[38] A SAR power image of the landslide and a coherence map are shown in Figure 7. Direct comparison with the optical image of Figure 1 is possible and shows a close correlation between areas with higher radar backscattering and areas without vegetation cover. The two main scarps and the Confinale stream, on the left flank of the landslide (on the right side of the image), are clearly distinguishable.

[39] Two sequences of interferograms (Table 3) are presented in Figures 8 and 9. The spatial resolution of the interferograms is the same as for the processed SAR images. The color of each pixel expresses the line-of-sight (LOS) component of the ground movement. The color scale has been converted to distance using the central frequency of observation.

[40] Displacements refer to a reference condition, corresponding to the time of acquisition of the first image in the sequence. Positive values indicate a movement toward the observer. If each image had been directly compared with the reference one, an additional procedure of phase unwrapping would be required since the displacements in some areas of the observed scene exceed half of the wavelength. In order to unambiguously assess displacements of several wavelengths, thus avoiding the necessity of an additional processing step, each interferogram has been obtained through a step-by-step procedure where phase differences are retrieved from pairs of images sequentially acquired and then are summed up to derive cumulated

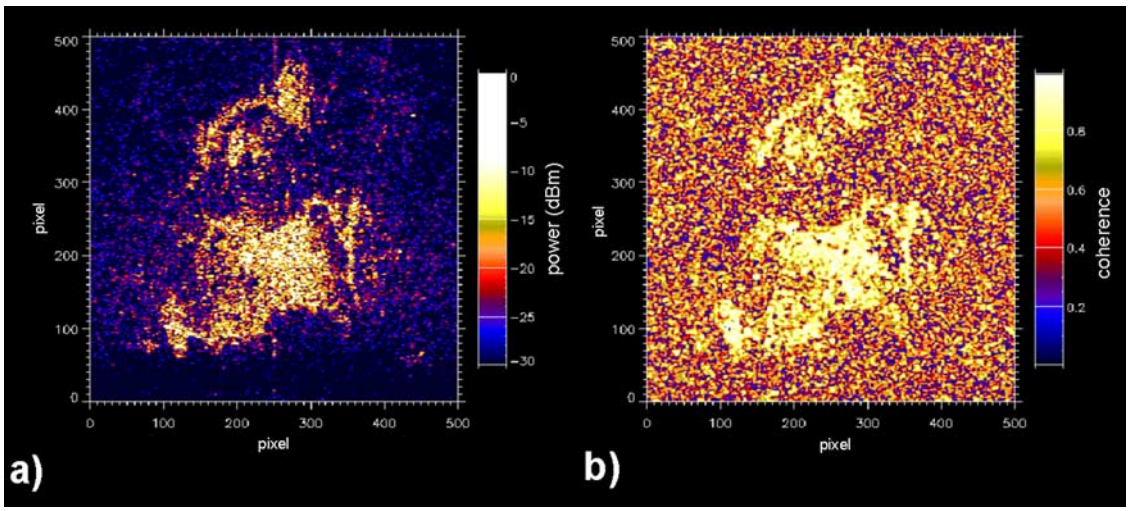

Figure 7. (a) Power image and (b) map of coherence of the slope.

Table 3. Details of the Sequences Obtained for the Ruinon Landslide

Sequence	Start		End		Number of Images	Number of Interferograms[a]	Effective Duration,[b] (h:min)
	Date	Time, UT	Date	Time, UT			
1	27 July 2000	1344	28 July 2000	0631	28	9	15:55
2	30 July 2000	2351	2 Aug 2000	0833	94	29	55:14

[a]Interferograms are obtained by averaging 3 or 4 consecutive images.
[b]The effective duration is the total time span between the first and the last averaged interferograms.

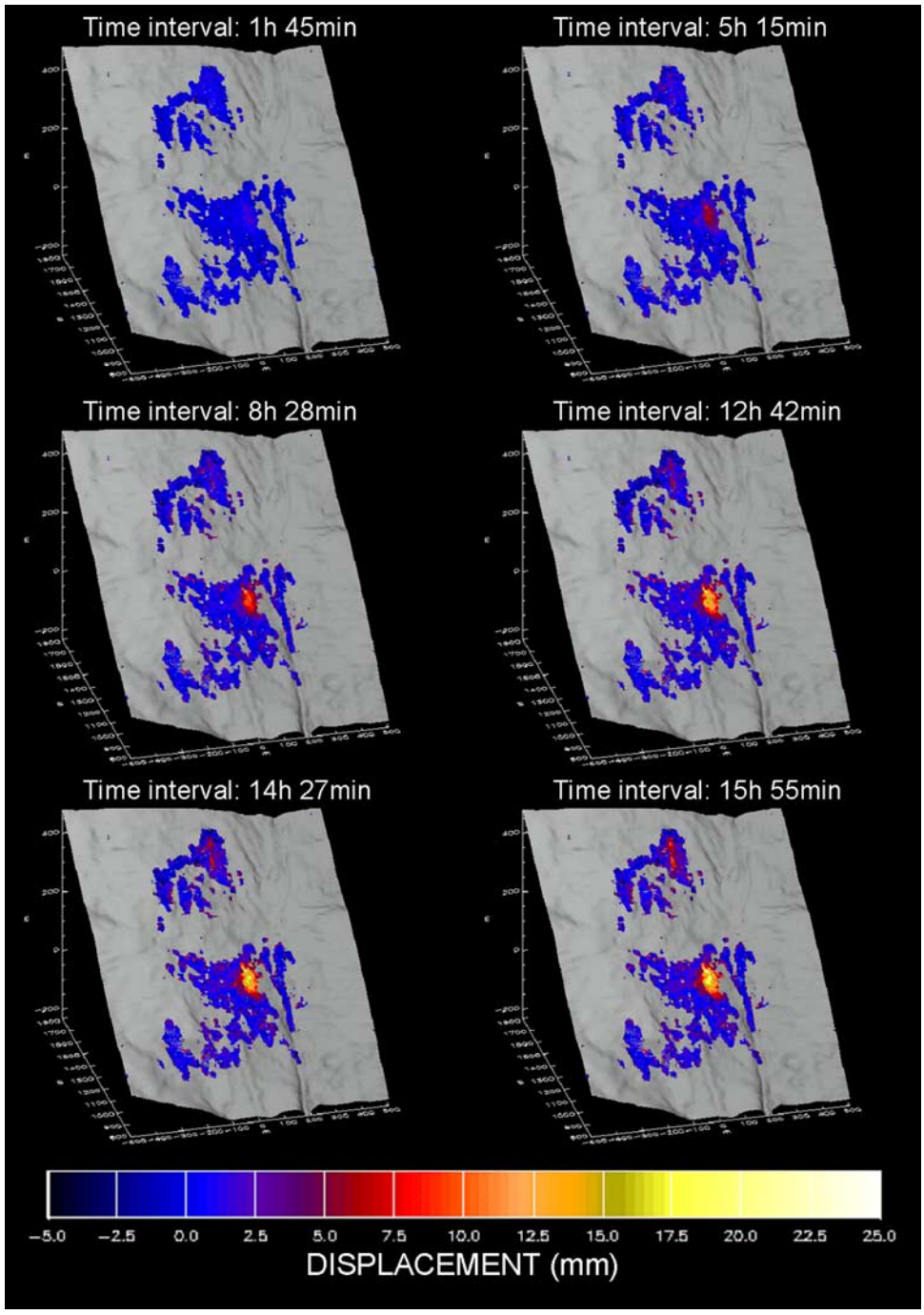

Figure 8. Selection of interferograms of the first sequence (starting time 27 July 2000, 1344 UT; effective duration, 15 hours 55 min).

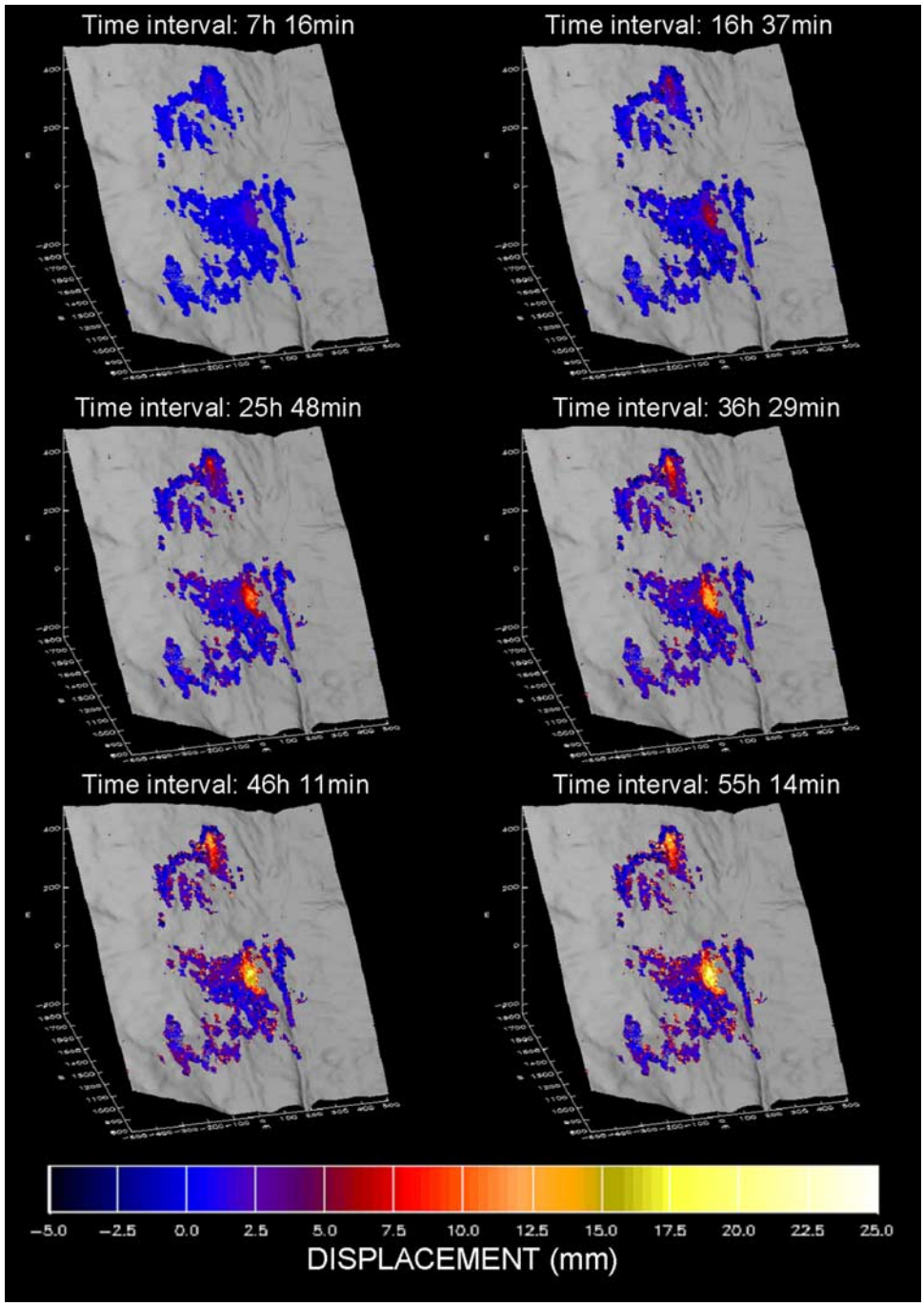

Figure 9. Selection of interferograms of the second sequence (starting time 30 July 2000, 2351 UT; effective duration, 55 hours 14 min).

displacements. A mask, derived from the analysis of the temporal evolution of the coherence, has been applied to the interferograms in order to eliminate pixels where the phase measurement is not reliable.

7. Discussion of Results

[41] The interpretation of the interferogram sequences, shown in Figures 8 and 9, highlights the presence of relevant displacements concentrated in well-defined areas within the landslide, with two relative maxima just beneath the two main scarps. The first sequence (Figure 8) shows significant displacements on the lower scarp from the second interferogram after 5 hours and 15 min. Movements affect an area of $\sim$100 $\times$ 100 m, with a subcircular shape. This area progressively enlarges in the successive interferograms, and displacements rise up to $\sim$21 mm at the end of the sequence (Figure 10), giving an average displacement rate of 1.32 mm h^{-1}. From the fourth interferogram, after 8 hours and 28 min, displacements start to occur also on the upper scarp, affecting an irregular area ($\sim$50 $\times$ 80 m) elongated along the dip direction of the slope. At the end

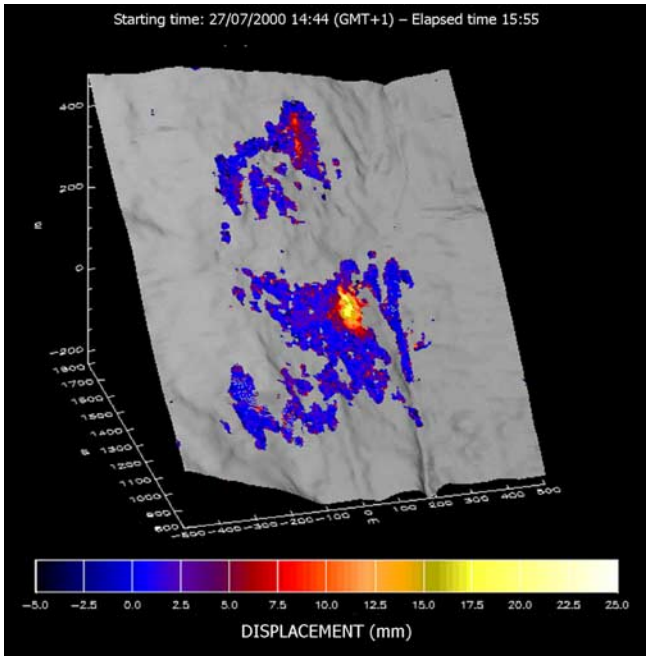

Figure 10. Enlargement of the last interferogram of the first sequence.

of the sequence (Figure 10) the maximum displacement measured in this area is ~12 mm (average displacement rate of 0.75 mm h^{-1}). The other parts of the slope seem to remain stable.

[42] The second sequence (Figure 9) shows similar movement patterns but with a lower rate. The subcircular area below the lower scarp is evident just from the first interferogram, and it maintains a symmetric displacement pattern with a central maximum of ~25 mm at the end of the sequence (Figure 11), which corresponds to an overall velocity of 0.45 mm h^{-1}. After a certain time the maximum displacement tends to remain constant while the moving zone progressively enlarges, as can be observed by comparing the last two interferograms of the sequence. The upper scarp is characterized by the same elongated unstable zone observed in the first sequence with a maximum displacement of 18 mm, corresponding to an average speed of 0.33 mm h^{-1}. The last interferogram (Figure 11) also shows some distributed displacements of lower magnitude, but their interpretation would require observation over a longer time span.

8. Validation of the Results

[43] The results have been validated by using independent measurements provided by the Geological Monitoring Centre of the Lombardia Region. The observed displacement patterns confirm the activity of the southeastern portion of the upper scarp, already documented by past monitoring data (G. Crosta et al., unpublished manuscript, 1999), whereas the large displacements recorded at the lower scarp were only hypothesized on the basis of geomorphic evidences but had never been assessed quantitatively.

[44] The position of all the available sensors placed on the landslide is shown in Figure 2. Several automatic extensometers are distributed along the upper scarp, and the area in which they show significant displacements exactly coincides with the one determined by radar measurements. The three extensometers with the highest and most coherent readings in the time period spanned by the radar sequence have been selected for validating the results. They are labeled E11a, E11b, and E16 in Figure 2. The comparison between the cumulated displacement, measured by these extensometers and by the radar in the corresponding pixels, is shown in Figure 12.

[45] Both the radar sensor and the extensometers assess only one component of the displacement vectors: The radar sensor assesses the displacements along the LOS, whereas each extensometer measures the component along the wire. The comparison was done projecting the radar-derived displacement in the direction of the extensometer wires.

[46] Extensometer readings, taken every 4 hours, are affected by cyclic effects (with a period of 24 hours) linked to daily temperature variations; this effect has been eliminated by plotting a six-point average versus time. The comparison between the radar measurements and the moving averages (Figure 13) shows a satisfactory agreement between the two independent techniques. With the exception of the extensometer E11a in the second sequence, characterized by a maximum discrepancy of ~4 mm, the difference between measurements over the total time interval is <1 mm, while discrepancies within this interval are limited to 2 mm.

[47] These discrepancies are, however, higher than the theoretical precision of the technique under the specific operational conditions in the field, which has been estimated to be 0.75 mm, due, probably, to the following reasons.

[48] (1) Radar measurements refer to an averaged displacement over a pixel of 5 × 5 m, while the extensometer provides point measurements. This could lead to either an

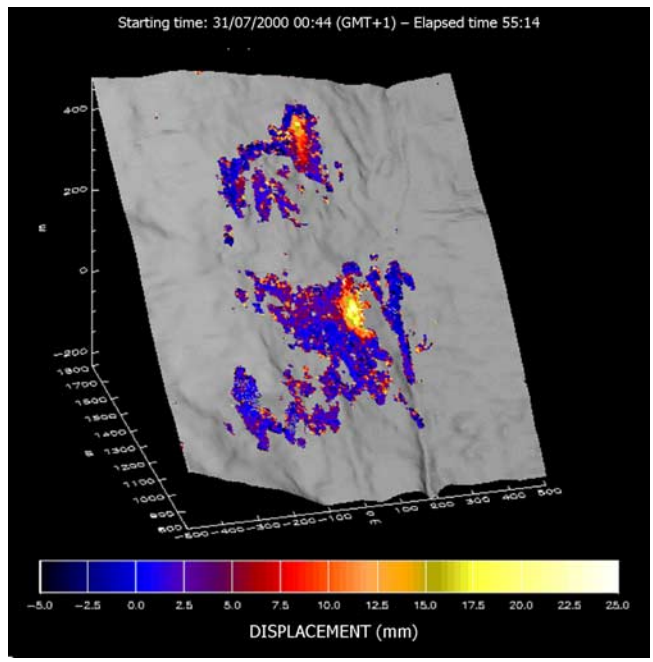

Figure 11. Enlargement of the last interferogram of the second sequence.

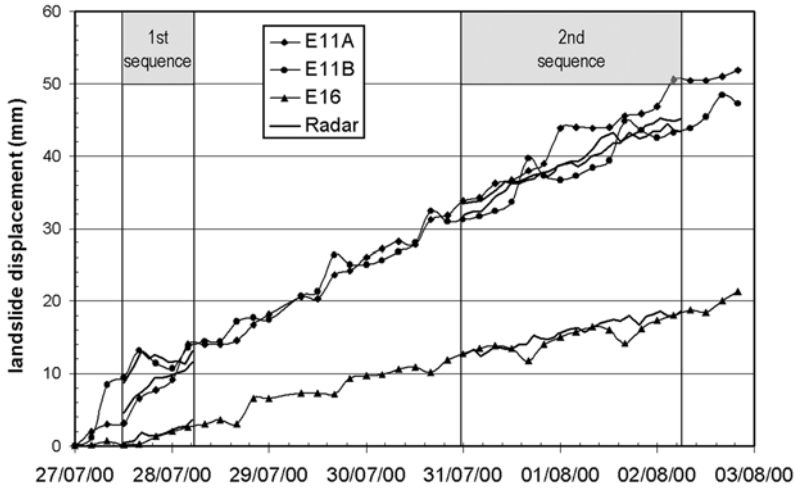

Figure 12. Cumulated displacements assessed by radar and by extensometers E11a, E11b, and E16 on the upper scarp.

overestimation or an underestimation depending on the general behavior of the other scattering centers located within the cell.

[49] (2) The positions of the three extensometers used for validation do not exactly correspond to the areas of maximum displacement detected by the radar. Instead, they are located on the border of these areas, where the gradient of the displacement field could be quite steep.

[50] (3) Radar data tend to average the displacement which occurs in the time interval necessary to acquire the image, whereas the extensometer readings are instantaneous. This could lead to an underestimation.

[51] (4) Small errors in assessing the angle between the radar LOS and the extensometer basis could lead to discrepancies in the comparison. This is probably true in the case of extensometer E11a, the data of which are systematically underestimated by radar measurements.

[52] Regarding the lower scarp, it is only possible to compare the average displacement rates assessed by radar and the periodic topographic measures on benchmarks since no automatic instrument is installed there. Most of benchmarks are positioned outside the area where the radar detects the maximum displacements. Measurements were carried out in the period between 27 July 2000 and 29 September 2000, showing an average velocity of 1.25 mm h^{-1} at the B6 benchmark (Figure 2). During the period between 25 July 2000 and 2 August 2000 the average displacement rate, assessed by the radar, was 0.9 mm h^{-1}. Considering the characteristics of this comparison, the agreement between these values can be considered satisfactory.

9. Assessment of the Technique With Respect to Other Monitoring Methods

[53] Compared with traditional methods of geotechnical and topographic monitoring, the GB-DInSAR technique permits one to derive spatially distributed information, represented as deformation maps offering a complete picture of an easier and more reliable interpretation of the movement mechanism. In addition, it is not necessary to install benchmarks or other instrumentation in the target area, and this fact represents an invaluable advantage in the case of dangerous areas to which access may be not possible. All maintenance and security efforts can be concentrated only at the radar location, and the cost of data acquisition and interpretation is relatively lower, after the initial investment.

[54] Compared to interferometry from satellite SAR imagery, the use of ground-based sensors allows a higher spatial resolution and excellent accuracy and precision. The GB-DInSAR is applicable to a variety of ground conditions, such as steep slopes and narrow valleys, where satellite images are scarcely utilizable. Moreover, using ground-based instrumentation, the time interval between measurements can be customized, thus making possible the investigation of a wider spectrum of landslide velocities and ensuring reliable results even for fast-moving landslides; these kinds of phenomenon pose the most risk to public safety and building instability.

[55] On the other hand, the main drawbacks of this technique concern the following aspects: (1) the necessity of installing the device on stable ground in a location where the target area is completely visible; (2) the impossibility of obtaining information in densely vegetated areas, where the backscattered signal results are heavily disturbed; (3) the necessity of a preliminary gross estimate of ground displacement rates for the selection of the time interval between successive measures in order to avoid uncontrolled phase wrapping; and (4) the necessity of maintenance and a permanent power supply if the device is installed in the field for long periods.

10. Conclusions

[56] The campaign on the Ruinon landslide is the first case in which data collected with the GB-DInSAR technique have been validated through comparison with ground truth data provided by a series of independent techniques. Owing to the relevance of the phenomenon under observation and to the actual conditions in which measurements have been carried out, this experience can be considered as a test for the effective use of the technique in operational conditions.

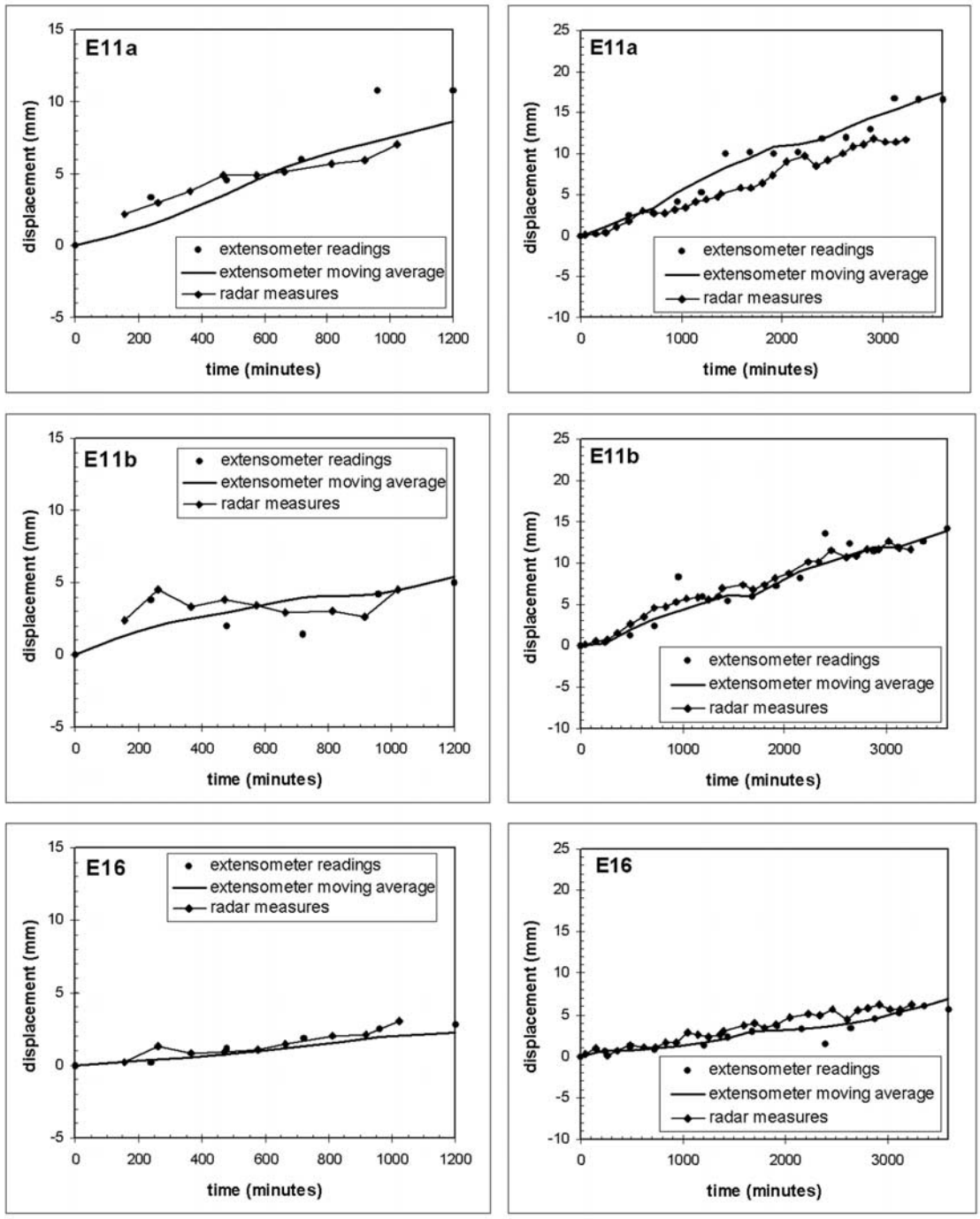

Figure 13. Detailed comparison between cumulated displacements assessed by radar and moving averages of extensometer readings. (top) Extensometer E11a. (middle) Extensometer E11b. (bottom) Extensometer E16. (left) First sequence; started on 27 July 2000, 1100 UT. (right) Second sequence; started on 30 July 2000, 2300 UT.

[57] In the specific case of the Ruinon landslide the technique allowed us to derive multitemporal displacement maps showing the LOS deformation field of the landslide and providing an immediate indication of the state and distribution of activity. These results have been achieved through a pure remote sensing technique, without installing sensors or benchmarks on the target area, and in difficult conditions from a logistical and operational point of view. The interpretation of the deformation fields obtained in the two interferogram sequences (15:55 and 55:15 hours long, respectively) allowed us to confirm the activity of the southeastern sectors of the upper scarp (already known on the basis of historical monitoring data) and of the lower scarp (only hypothesized on the basis of surface geological evidence and only partially verified through GPS and topographic surveys). In all cases, the comparison with the independent sensors can be considered satisfactory.

[58] The sequences of interferograms are, however, too short to improve our interpretation of the landslide mechanism. A clear picture of the landslide mechanism in space and time can be obtained only with long-term monitoring extended over several weeks or months. In the short spans covered by the radar campaign it was possible to assess the fastest movements related to the sliding of superficial debris. It is, however, significant how in selected points these movements are comparable with those assessed by extensometers across the upper scarp. The debris displacement occurs, probably, as a consequence of the deep-seated sliding of the landslide left block.

[59] If DInSAR performances could be confirmed, also, by long-term monitoring, this technique could be employed to better understand landslide mechanisms, especially in the case of large-scale and complex mass movements with an irregular distribution of activity, such as the Ruinon landslide. The capability of the system to provide two-dimensional data can be helpful in interpreting the landslide kinematics and in providing input for numerical models. Moreover, long time series of SAR-derived displacements, assessed over wide landslide sectors, could be directly used for prediction and early warning purposes, applying models for forecasting the timing of slope failure such as the ones presented by *Fukuzono* [1985] or by *Voight* [1988].

[60] Balancing the advantages and disadvantages discussed in section 9, it is possible to affirm that the proposed portable instrumentation can be effectively utilized for the following applications: (1) for the study and interpretation of slope instability mechanisms in space and time; (2) for landslide control in urban areas, cultural heritage sites, and other locations of high societal value; (3) for the design of alarm and early warning systems for civil protection purposes; and (4) to test the effectiveness of landslide stabilization works through time.

[61] **Acknowledgments.** Research on the applicability of ground-based SAR for landslide monitoring is sponsored by the Italian Space Agency (ASI) and by the National Research Council Group for Hydro-Geological Disaster Prevention (CNR-GNDCI), supported by the Italian Department of Civil Protection. In particular, this activity is part of the ASI program "Remote-Sensing Techniques for Monitoring Landslides" and of the AMHARAL project "Analytical Methods for the Definition of Hazard Areas for Rainfall-Induced Landslides." Part of the activity has been developed within the GNDCI-MOGEM project "Monitoring High Risk Slope Movements." The application to the Ruinon landslide was carried out in the frame of a research contract between the Lombardia Regional Administration and the University of Firenze "Testing ground-based SAR interferometry for monitoring the Ruinon landslide in Valfurva." The Geological Monitoring Centre of the Lombardia Region, and particularly G. Mannucci and S. Tavelli, are acknowledged for providing validation data and support to the measurement campaign. The Mayor of Valfurva is acknowledged for his practical support of the measurement campaign. A special thanks is due to M. Basso of the JRC who is responsible for the setup, installation, and maintenance of LISA. Guido Luzi and Massimiliano Pieraccini of the Department of Electronics and Telecommunications at the University of Florence are acknowledged for having taken part in the field campaign of measurements. The doctoral and postdoctoral group of the University of Florence, namely A. Del Piccolo, C. Picone, F. Bianchi, S. Dapporto, G. Falorni, and G. De Rosa, gave effective support for the organization and implementation of the campaign. F. Catani and C. Picone are responsible for the production of the digital elevation model. This is CNR-GNDCI publication 2512.

References

Achache, J., B. Fruneau, and C. Delacourt, Applicability of SAR interferometry for operational monitoring of landslides, paper presented at the 2nd ERS Applications Workshop, Eur. Space Agency, London, 1995.

Agliardi, F., G. Crosta, and A. Zanchi, Structural constraints on deep-seated slope deformation kinematics, *Eng. Geol.*, *59*, 1–2, 83–102, 2001.

Atzeni, C., M. Basso, P. Canuti, N. Casagli, D. Leva, G. Luzi, S. Moretti, M. Pieraccini, A. J. Sieber, and D. Tarchi, Ground-based SAR interferometry for landslide monitoring and control, paper presented at the Field Workshop on Landslides and Natural/Cultural Heritage, Intl. Soc. Soil Mech. and Geotech. Eng., Trabzon, Turkey, 25–26 Aug. 2001a.

Atzeni, C., P. Canuti, and D. Tarchi, Monitoring unstable cultural heritage sites with radar interferometry, in *UNESCO/IGCP Symposium on Landslide Risk Mitigation and Protection of Cultural and Natural Heritage*, edited by K. Sassa, pp. 257–264, Kyoto Univ., Japan, 2001b.

Atzeni, C., P. Canuti, N. Casagli, D. Leva, G. Luzi, S. Moretti, M. Pieraccini, A. J. Sieber, and D. Tarchi, A portable device for landslide monitoring using radar interferometry, *Landslide News Intl. Newsl.*, *14/15*, 19–22, 2003.

Beatrizotti, G., G. Chiesi, L. Scesi, and D. Tarchi, Il monitoraggio della frana che minaccia il Comune di Airolo (Svizzera), paper presented at the International Congress, GeoBen, Torino, Italy, 2000.

Carnec, C., D. Massonnet, J. P. Villain, and C. King, Potential application of differential SAR interferometry for monitoring impact of underground mining, paper presented at the 1st Workshop on SAR Interferometry, Earth Sci. and Technol. Organ., Tokyo, 1994.

Carnec, C., C. King, and D. Massonnet, Measurement of land subsidence by means of differential SAR interferometry, in *Proceedings of the 5th International Symposium on Land Subsidence (FISOLS95)*, edited by B. J. Barends et al., pp. 139–148, A. A. Balkema, Brookfield, Vt., 1995.

Carnec, C., D. Massonnet, and C. King, Two examples of the use of SAR interferometry on displacement fields of small spatial extent, *Geophys. Res. Lett.*, *23*, 3579–3582, 1996.

Cruden, D. M., A simple definition of a landslide, *Bull. Int. Assoc. Eng. Geol.*, *43*, 27–29, 1991.

Cruden, D. M., and D. J. Varnes, Landslides types and processes, in *Landslides: Investigation and Mitigation*, *Spec. Rep. 247*, pp. 36–75, Transp. Res. Board, Natl. Res. Counc., Natl. Acad. Press, Washington, D. C., 1996.

Curlander, J. C., and R. N. McDonough, *Synthetic Aperture Radar: Systems and Signal Processing*, 672 pp., John Wiley, Hoboken, N. J., 1991.

Del Piccolo, A., Frana del Ruinon (Valfurva, Sondrio): Aspetti geomorfologici e geotecnici, thesis, Earth Sci. Dep., Univ. of Firenze, Italy, 1999.

Ferretti, A., C. Prati, and F. Rocca, Monitoring terrain deformations using multi-temporal SAR images, paper presented at Proceedings '99, Comm. on Earth Observ. Satell., Toulouse, France, 26–29 Oct. 1999a.

Ferretti, A., C. Prati, and F. Rocca, Permanent scatterers in SAR interferometry, paper presented at the International Geoscience and Remote Sensing Symposium, Geosci. and Remote Sens. Soc., Hamburg, Germany, 28 June to 2 July 1999b.

Ferretti, A., C. Prati, and F. Rocca, Non-linear subsidence rate estimation using permanent scatterers in differential SAR interferometry, *IEEE Trans. Geosci. Remote Sens.*, *38*(5), 2202–2212, 2000.

Ferretti, A., C. Prati, and F. Rocca, Permanent scatterers in SAR interferometry, *IEEE Trans. Geosci. Remote Sens.*, *39*(1), 8–20, 2001.

Fornaro, G., G. Franceschetti, and R. Lanari, Interferometric SAR phase unwrapping techniques: A comparison, *J. Opt. Soc. Am.*, *34*, 2355–2366, 1996.

Fortuny, J., and A. J. Sieber, Fast algorithm for a near-field synthetic aperture radar processor, *IEEE Trans. Antennas Propag.*, *42*, 1458–1460, 1994.

Fruneau, B., J. Achache, and C. Delancourt, Observation and modelling of the Saint-Etienne-de-Tinee landslide using SAR interferometry, *Tectonophysics*, *265*, 181–190, 1996.

Fukuzono, T., A method to predict the time of slope failure caused by rainfall using the inverse number of velocity of surface displacement, *J. Jpn. Landslide Soc.*, *22*(2), 8–13, 1985.

Gabriel, A. K., R. M. Goldstein, and H. A. Zebker, Mapping small elevation changes over large areas: Differential radar interferometer, *J. Geophys. Res.*, *94*, 9183–9191, 1989.

Goldstein, R. M., H. A. Zebker, and C. L. Werner, Satellite radar interferometry: Two-dimensional phase unwrapping, *Radio Sci.*, *23*(4), 713–720, 1988.

Goldstein, R. M., H. Engelhardt, B. Kamb, and R. M. Frolich, Satellite radar interferometry for monitoring ice-sheet motion: Application to an Antarctic ice stream, *Science*, *262*, 1525–1530, 1993.

Kimura, H., and Y. Yamaguchi, Detection of landslide areas using radar interferometry, *Photogramm. Eng. Remote Sens.*, *66*(3), 337–344, 2000.

Massonnet, D., M. Rossi, C. Carmona, F. Adragna, G. Peltzer, K. Feigl, and T. Rabaute, The displacement field of the Landers earthquake mapped by radar interferometry, *Nature*, *364*, 138–142, 1993.

Massonnet, D., K. Feigl, M. Rossi, and F. Adragna, Radar interferometric mapping of deformation in the year after the Landers earthquake, *Nature*, *369*, 227–230, 1994.

Massonnet, D., P. Briole, and A. Arnaud, Deflation of Mount Etna monitored by space radar interferometry, *Nature*, *375*, 567–570, 1995.

Peltzer, G., K. W. Hudnut, and K. L. Feigl, Analysis of coseismic surface displacement gradients using radar interferometry: New insights into the Landers earthquake, *J. Geophys. Res.*, *99*, 21,971–21,981, 1994.

Pieraccini, M., D. Tarchi, H. Rudolf, D. Leva, G. Luzi, and C. Atzeni, Interferometric radar for remote monitoring of building deformations, *Electron. Lett.*, *36*(6), 569–570, 2000a.

Pieraccini, M., D. Tarchi, H. Rudolf, D. Leva, G. Luzi, G. Bartoli, and C. Atzeni, Structural static testing by interferometric synthetic radar, *NDTandE Intl.*, *33*(8), 565–570, 2000b.

Prati, C., F. Rocca, and A. Monti Guarnieri, Monitoring surface deformations with SAR interferometry, paper presented at the International Symposium on Retrieval of Bio- and Geophysical Parameters From SAR Data for Land Applications, Cent. Natl. d'Etud. Spatiales-Eur. Space Agency, Toulouse, France, 1995.

Refice, A., F. Bovenga, J. Wasowski, and L. Guerriero, Use of InSAR Data for landslide monitoring: A case study from southern Italy, paper presented at the International Geoscience and Remote Sensing Symposium, Geosci. and Remote Sens. Soc., Honolulu, Hawaii, 2000.

Rizzo, V., and M. Tesauro, SAR interferometry and field data of Randazzo landslide (eastern Sicily, Italy), *Phys. Chem. Earth, Part B*, *25*, 771–780, 2000.

Rosen, P. A., S. Hensley, I. R. Joughin, F. K. Li, S. N. Madsen, E. Rodriguez, and R. M. Goldstein, Synthetic aperture radar interferometry, *Proc. IEEE*, *88*(3), 333–382, 2000.

Rott, H., and A. Siegel, Analysis of mass movements in Alpine terrain by means of SAR interferometry, paper presented at the International Geoscience and Remote Sensing Symposium, Geosci. and Remote Sens. Soc., Hamburg, Germany, 28 June to 2 July 1999.

Rott, H., B. Scheuchel, A. Siegel, and B. Grasemann, Monitoring very slow slope movements by means of SAR interferometry: A case study from a mass waste above a reservoir in the Ötztal Alps, Austria, *Geophys. Res. Lett.*, *26*(11), 1629–1632, 1999.

Rott, H., C. Mayer, and A. Siegel, On the operational potential of SAR interferometry for monitoring mass movements in alpine areas, paper presented at the European Conference on Synthetic Aperture Radar, Coop. Res. Cent. for Sensor Signal and Inf. Process., Munich, Germany, 22–25 May 2000.

Rudolf, H., and D. Tarchi, LISA: The linear SAR instrument, *Tech. Rep. I. 99. 126*, Eur. Comm. Joint Res. Cent., Ispra, Italy, 1999.

Rudolf, H., D. Leva, D. Tarchi, and A. J. Sieber, A mobile and versatile SAR system, paper presented at the International Geoscience and Remote Sensing Symposium, Geosci. and Remote Sens. Soc., Hamburg, Germany, 28 June to 2 July 1999.

Singhroy, V., and K. Mattar, SAR image techniques for mapping areas of landslides, paper presented at the 19th Conference, Intl. Soc. for Photogramm. and Remote Sens., Amsterdam, 2000.

Singhroy, V., K. Mattar, and L. Gray, Landslide characterization in Canada using interferometric SAR and combined SAR and TM images, *Adv. Space Res.*, *2*(3), 465–476, 1998.

Tarchi, D., E. Ohlmer, and A. J. Sieber, Monitoring of structural changes by radar interferometry, *Res. Nondestructive Eval.*, *9*, 213–225, 1997.

Tarchi, D., H. Rudolf, G. Luzi, L. Chiarantini, P. Coppo, and A. J. Sieber, SAR interferometry for structural change detection: A demonstration test on a dam, paper presented at the International Geoscience and Remote Sensing Symposium, Geosci. and Remote Sens. Soc., Hamburg, Germany, 28 June to 2 July 1999.

Tarchi, D., H. Rudolf, M. Pieraccini, and C. Atzeni, Remote monitoring of buildings using a ground-based SAR: Application to cultural heritage survey, *Int. J. Remote Sens.*, *21*(18), 3545–3551, 2000a.

Tarchi, D., D. Leva, and A. J. Sieber, SAR interferometric techniques from ground based system for the monitoring of landslides, paper presented at the International Geoscience and Remote Sensing Symposium, Geosci. and Remote Sens. Soc., Honolulu, Hawaii, 2000b.

Tarchi, D., N. Casagli, R. Fanti, D. Leva, G. Luzi, A. Pasuto, M. Pieraccini, and S. Silvano, Landslide monitoring by using ground-based SAR interferometry: An example of application to the Tessina landslide in Italy, *Eng. Geol.*, *68*, 15–30, 2003.

Voight, B., Material science law applies to time forecast of slope failure, *Landslide News Intl. Newsl.*, *3*, 8–11, 1988.

Wasowski, J., and P. Gostelow, Engineering geology landslide investigations and SAR interferometry, paper presented at the Proceedings of the 2nd International Workshop on ERS SAR Interferometry, FRINGE 1999, Eur. Space Agency, Liege, Belgium, 10 –12 Nov. 1999.

Wiesbeck, W., and D. Kähny, Single reference three target calibration and error correction for monostatic polarimetric free space measurements, *Proc. IEEE*, *79*, 1551–1558, 1991.

Williams, S., Y. Bock, and P. Fang, Integrated satellite interferometry: Tropospheric noise, GPS estimates, and implications for interferometric synthetic aperture radar products, *J. Geophys. Res.*, *103*, 27,051–27,068, 1998.

Zebker, H. A., and R. M. Goldstein, Topographic mapping from interferometric synthetic aperture radar observations, *J. Geophys. Res.*, *91*, 4993–4999, 1986.

N. Casagli and S. Moretti, Earth Sciences Department, University of Florence, Via La Pira n.4, I-50121 Florence, Italy. (nicola.casagli@unifi.it; smoretti@geo.unifi.it)

D. Leva, A. J. Sieber, and D. Tarchi, European Commission, Joint Research Centre, Institute for the Protection and Security of the Citizen, Via E. Fermi n.1, I-21020 Ispra, Italy. (davide.leva@jrc.it; alois.sieber@jrc.it; dario.tarchi@jrc.it)